$\pi\pi$ Scattering Length Measurements from Ke4 and $K^{\pm} \to \pi^{\pm}\pi^0\pi^0$ Decays at NA48/2

F. Bucci

Abstract We report here the preliminary results on the $\pi\pi$ scattering lengths a_0 and a_2 at NA48/2. We determine a_0 and a_2 by studying two different kaon decay modes. In the $K^{\pm} \to \pi^+\pi^- e^{\pm}\nu$ decays (K_{e4}) we measure the form factors of the hadronic current (F, G, H) and the $\pi\pi$ phase difference ($\delta = \delta_s - \delta_p$) in ten independent bins of the $\pi\pi$ mass spectrum to investigate their variation. Taking into account the isospin simmetry breaking effects and using numerical solutions of the Roy equations we obtain a_0 and a_2. In the $K^{\pm} \to \pi^{\pm}\pi^0\pi^0$ events we determine the $a_0 - a_2$ difference and a_2 from a fit to the $\pi^0\pi^0$ invariant mass distribution (M_{00}) around $M_{00} = 2m_{\pi^+}$.

Keywords: Charged kaon, cusp, Ke4, scattering length

1 Introduction

The single-flavor quark condensate $< 0|\overline{q}q|0 >$ is a fundamental parameter of the chiral perturbation theory (ChPT), determining the relative size of mass and momentum terms in the expansion. Since it cannot be predicted theoretically, its value must be experimentally determined by measuring, for example, the $\pi\pi$ scattering lengths a_0 and a_2 whose values are precisely predicted within the framework of the ChPT, assuming a big quark condensate [1], or of a generalised ChPT, where the quark condensate is a free parameter [2].

The K_{e4} decay is a very clean environment for the measurement of the $\pi\pi$ scattering lengths since the two pions are the only hadrons in the final state and they are produced close to the threshold. In the past years, only two experiments collected significant samples of K_{e4} decays [3,4], large enough to study their properties

F. Bucci
Università di Firenze, via G. Sansone 1, 50019 Sesto Fiorentino, Firenze,
e-mail: francesca.bucci@fi.infn.it

V. Begun et al. (eds.), *Progress in High-Energy Physics and Nuclear Safety*,

but without reaching the same precision level as the theoretical predictions. An alternative way to study the $\pi\pi$ interactions through a measurement of the lifetime of the $\pi\pi$-atom was followed in the DIRAC experiment at CERN [1]. An additional method for the determination of the $\pi\pi$ scattering length a_2 and the $a_0 - a_2$ difference is based on the study of the $\pi^0\pi^0$ invariant mass spectrum in the $\boldsymbol{K}^{\pm} \to \pi^{\pm}\pi^0\pi^0$ decays.

We present here the preliminary results on $\pi\pi$ scattering lengths based on about $1.2 \cdot 10^6$ K_{e4} events and $6 \cdot 10^7$ $\boldsymbol{K}^{\pm} \to \pi^{\pm}\pi^0\pi^0$ decays collected by the NA48/2 experiment.

2 Experimental setup

The NA48/2 experiment beam line has been designed to measure the CP violating charged asymmetry in the $K \to 3\pi$ decay [6]. Simultaneous K^+ and K^- beams are produced by 400 GeV protons from the CERN Super Proton Synchrotron (SPS) impinging on a beryllium target. Kaons are deflected in a front-end achromat to select the momentum band of (60 ± 3) GeV/c and then focused at the beginning of the detector $\sim$200 m downstream, at the end of the $\sim$100m long decay region. The NA48 detector and its performances are described in detail elsewhere [7]. The K_{e4} analysis is essentially based on the magnetic spectrometer, consisting of four drift chambers and a dipole magnet located between the second and the third chamber. Each chamber consists of four staggered double planes of sense wires along the horizontal, vertical and $\pm 45^\circ$ directions. The momentum resolution of the spectrometer is $\sigma_p/p = (1.02 \oplus 0.044 \cdot p)\%$ (with p in GeV/c). The $\boldsymbol{K}^{\pm} \to \pi^{\pm}\pi^0\pi^0$ analysis uses the liquid-krypton calorimeter (LKr) to identify the photons produced in the π^0 decay. The transverse segmentation and the 27 radiation lenght thickness result in an energy resolution $\sigma_E/E = (3.2/\sqrt{E} \oplus 9.0/E \oplus 0.42)\%$ (with E in GeV) and a space resolution for isolated showers $\sigma_x = \sigma_y = (0.42/\sqrt{E} \oplus 0.06)$ cm (with E in GeV). Furthermore, a hodoscope consisting of two planes of scintillators segmented into horizontal and vertical strips is used to trigger the detector readout on charged track topologies. Its time resolution is $\sim$150 ps.

3 The K_{e4} decay

3.1 Formalism

The kinematics of the K_{e4} decay is fully described by five variables introduced by Cabibbo and Maksymowicz [8]: $M^2_{\pi\pi}$, the squared invariant mass of the dipion system; $M^2_{e\nu}$, the squared invariant mass of the dilepton; θ_π, the angle of the pion with the same charge as the kaon in the dipion rest frame ($\Sigma_{\pi\pi}$) with respect to

the direction of flight of the dipion in the K rest frame (Σ_K); θ_e, the angle of the electron in the dilepton rest frame ($\Sigma_{e\nu}$) with respect to the direction of flight of the dilepton system in Σ_K; ϕ, the angle between the plane formed by the two pions and the corresponding plane formed by the two leptons. Three axial (F, G, R) and one vector (H) dimensionless complex form factors contribute to the transition amplitude and can be developed in partial wave expansions of s, p, d waves [9]:

$$\begin{aligned} F &= F_s e^{i\delta_s} + F_p e^{i\delta_p} + d\ wave \\ G &= G_p e^{i\delta_p} + d\ wave \\ H &= H_p e^{i\delta_p} + d\ wave \end{aligned} \tag{1}$$

where we assumed the same phase for F_p, G_p and H_p. The third axial form factor R is suppressed by a factor $m_e^2/M_{e\nu}^2$. Neglecting d wave terms, F_s, F_p, G_p and H_p can be further [10] expanded in powers of $q^2 = (M_{\pi\pi}^2/4m_\pi^2) - 1$:

$$\begin{aligned} F_s &= f_s + f_s^{'} q^2 + f_s^{''} q^4 + ... \\ F_p &= f_p + f_p^{'} q^2 ... \\ G_p &= g_p + g_p^{'} q^2 + ... \\ H_p &= h_p + h_p^{'} q^2 ... \end{aligned} \tag{2}$$

3.2 Selection and fitting procedure

The K_{e4} events are selected by requiring three charged tracks within the detector acceptance. Two opposite sign pions and one electron or positron are required. Particle identification is mainly based on the E/p ratio between the energy as measured by the LKr calorimeter and the momentum as measured by the magnetic spectrometer. The reconstructed three tracks invariant mass (assigning a pion mass to each track) and the transverse momentum p_t relative to the beam axis have to be outside an ellipse centered on the kaon mass and zero p_t, allowing missing energy and p_t for the undetected neutrino. The kaon momentum p_K is obtained by imposing energy-momentum conservation in the Ke4 decay, under the assumption of an undetected neutrino and fixing the kaon mass and the beam direction to their nominal value. If a solution exists in the range between 50 and 70 GeV/c, the event is kept and the solution closer to 60 GeV/c is assigned to p_K. The background comes from $K^{\pm} \to \pi^+\pi^-\pi^{\pm}$ decays with a pion misidentified as an electron or the subsequent $\pi \to e\nu$ decay and $K^{\pm} \to \pi^{\pm}\pi^0(\pi^0)$ decays with $\pi^0 \to e^+e^-\gamma$, an electron misidentified as a pion and photon(s) undetected. The background is evaluated by studying the "wrong-sign" events, i.e. events for which the $\Delta S = \Delta Q$ rule is violated (the electron charge is opposite to the total one) and it results to be at 0.5% level.

We define 15,000 iso-populated boxes in the 5-dimension space of $M_{\pi\pi}$, M_{ev}, $cos\theta_\pi$, $cos\theta_e$ and ϕ. The form factors F_s, F_p, G_p, H_p and the phase shift $\delta = \delta_s - \delta_p$ are extracted by minimizing a log-likelihood estimator in the ten independent $M_{\pi\pi}$ bins. Actually, only relative form factors F_p/F_s, G_p/F_s and H_p/F_s are accessible since the branching fraction is not measured. Their variation with $M_{\pi\pi}$ is then fitted to extract the form factors $f_s^{'}/f_s$, $f_s^{''}/f_s$, $f_e^{'}/f_s$, f_p/f_s, g_p/f_s, $g_p^{'}/f_s$ and h_p/f_s.

3.3 Results

Preliminary results on form factors data are shown in Table 1. The systematic errors are quoted by comparing two independent analysis and taking into account the effect of reconstruction method, acceptance, fit method, uncertainty on background estimate, electron-ID efficiency, radiative corrections and bias due to the neglected M_{ev} dependence.

Dispersion relations and data at intermediate energies give the functional relation between the phase shift δ and $M_{\pi\pi}$ with the scattering lenghts a_0 and a_2 as parameters [11–13]. Figure 1 shows the measured variation of δ with $M_{\pi\pi}$. After correcting for the isospin simmetry breaking effects, the a_0 and a_2 values are extracted by performing a fit to the phase shift variation. The $\pi\pi$ scattering data above 0.8 GeV and the dispersion relations restrict the a_0 and a_2 values to a band in the (a_0, a_2) plane called the Universal Band (UB); the width of the allowed band is considerably reduced if the $a_2 = f(a_0)$ relation given by the chiral perturbation theory [14] is imposed in addition. Exploiting the ChPT constraint, $a_2 = f(a_0)$, we also perfom a one paramater fit. Fit results are reported in Table 2.

Table 1 Form factors preliminary results based on $1.2 \cdot 10^6$ K_{e4} events

				Stat		Syst
$f_s^{'}/f_s$	=	0.158	±	0.007	±	0.006
$f_s^{''}/f_s$	=	−0.078	±	0.007	±	0.007
$f_e^{'}/f_s$	=	0.067	±	0.006	±	0.009
f_p/f_s	=	−0.049	±	0.003	±	0.004
g_p/f_s	=	0.869	±	0.010	±	0.012
$g_p^{'}/f_s$	=	0.087	±	0.017	±	0.015
h_p/f_s	=	−0.402	±	0.014	±	0.008

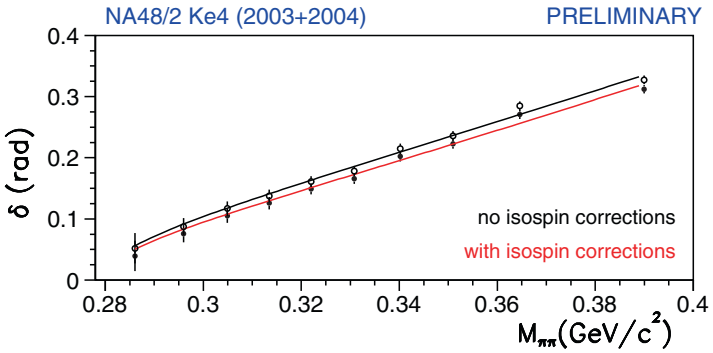

Fig. 1 Phase shift variation as a function of $M_{\pi\pi}$ with (full circle) and without (empty circle) taking into account the isospin symmetry breaking effects

Table 2 Scattering lengths preliminary results on $1.2 \cdot 10^6$ K_{e4} events

Without ChPT constraint	With ChPT constraint
$a_0 m_{\pi^+} = 0.218 \pm 0.013_{stat} \pm 0.007_{syst}$ $a_2 m_{\pi^+} = -0.0457 \pm 0.0084_{stat} \pm 0.0041_{syst}$	$a_0 m_{\pi^+} = 0.220 \pm 0.005_{stat} \pm 0.002_{syst}$

4 The $K^{\pm} \to \pi^{\pm}\pi^0\pi^0$ decay

4.1 The cusp effect

The study of $2.4 \cdot 10^7$ $K^{\pm} \to \pi^{\pm}\pi^0\pi^0$ decays showed a change of slope in the squared invariant mass distribution of the $\pi^0\pi^0$ system (M_{00}) at the $\pi^+\pi^-$ threshold [15]. This anomaly, never observed in the previous experiments, was theoretically interpreted as an effect due to the charge-exchange scattering process $\pi^+\pi^- \to \pi^0\pi^0$ in $K^{\pm} \to \pi^{\pm}\pi^+\pi^-$ decays. Cabibbo [16] proposed a simple rescattering model desribing the $K^{\pm} \to \pi^{\pm}\pi^0\pi^0$ decay amplitude as the sum of two terms: the unperturbed decay amplitude $\mathscr{M}_0$ and the contribution $\mathscr{M}_1$ from the $K^{\pm} \to \pi^{\pm}\pi^+\pi^-$ decay amplitude through the $\pi^+\pi^- \to \pi^0\pi^0$ charge-exchange with the renormalization condition $\mathscr{M}_1 = 0$ at $M_{00} = m_{\pi^+\pi^-}$. $\mathscr{M}_1$ is proportional to $a_0 - a_2$ and changes from real to imaginary at the $\pi^+\pi^-$ threshold with the consequence that it interferes destructively with $\mathscr{M}_0$ below the threshold while it adds quadratically above it. The experimental measurement of this effect thus provides a precise determination of $a_0 - a_2$ (including its sign). Subsequently, Cabibbo and Isidori (CI) [17] have extended the amplitude calculation at two loops level adding five terms proportional to the scattering lenghts. This model allows to extract $a_0 - a_2$ and a_2. A different model was developed by Colangelo et al. (CGKR) [18] which includes the electromagnetic effects and introduces a different correlation between the parameters with respect to the CI approach.

4.2 Selection and fitting procedure

The analysis was redone on $6 \cdot 10^7$ $K^{\pm} \to \pi^{\pm}\pi^0\pi^0$ decays. Signal events are selected by requiring one charged track and at least four energy clusters in the LKr. We assume that each possible pair of photons originates from $\pi^0 \to \gamma\gamma$ and we calculate the longitudinal position of the corresponding neutral vertex. We choose the two vertices combination with the closest vertices and the arithmetic average of the two π^0 vertices is taken as the kaon decay vertex. This choice gives the best M_{00} resolution at $M_{00} = 2m_{\pi^+}$. The r.m.s. of the M_{00}^2 resolution curve increases with M_{00}^2, varying between $\sim$0.0002 GeV^2 and $\sim$0.001 GeV^2. The cusp in the M_{00}^2 distribution is clearly visible in Fig. 2 at $M_{00} = 2m_{\pi^+}$. At this point the resolution on M_{00}^2 is $\sim$0.0003 GeV^2.

Both the CI and CGKR formulations are used to fit the squared invariant mass distribution of the $\pi^0\pi^0$ system. The resolution and the detector response matrix are obtained using an accurate Geant3 based simulation. For the unperturbed amplitude $\mathcal{M}_0$ the PDG parameterization is taken:

$$\mathcal{M}_0 = A_0(1 + \frac{1}{2}g_0 u + \frac{1}{2}h_0' u^2 + \frac{1}{2}k_0' v^2) \tag{3}$$

where u and v are the Dalitz variables.

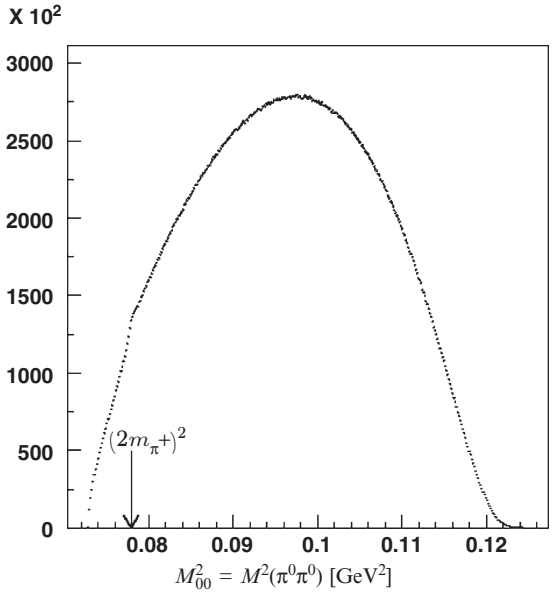

Fig. 2 $\pi^0\pi^0$ invariat mass distribution in $K^{\pm} \to \pi^{\pm}\pi^0\pi^0$ decays. A cusp at $M_{00} = 2m_{\pi^+}$ is clearly visible

The fit parameters are g_0, $h_0^{'}$, $a_0 - a_2$, a_2 and the normalization factor N. $k_0^{'}$ and the unperturbed amplitude of the $K^{\pm} \to \pi^{\pm}\pi^+\pi^-$ decay which is present in $\mathscr{M}_1$ are fixed to the values previously measured by NA48/2 [19]. The fit is performed excluding a small region around the threshold where the theoretical treatment of the electromagnetic interaction is still missing.

4.3 Results

The preliminary results obtained on $6 \cdot 10^7$ $\boldsymbol{K}^{\pm} \to \pi^{\pm}\pi^0\pi^0$ events are:

$$\begin{aligned}
CI \quad &: (a_0 - a_2) m_{\pi^+} = \quad 0.266 \pm 0.005_{stat} \pm 0.002_{syst} \pm 0.001_{ext} \\
&\quad a_2 \; m_{\pi^+} = -0.039 \pm 0.009_{stat} \pm 0.006_{syst} \pm 0.002_{ext} \\
CGKR &: (a_0 - a_2) m_{\pi^+} = \quad 0.273 \pm 0.005_{stat} \pm 0.002_{syst} \pm 0.001_{ext} \\
&\quad a_2 \; m_{\pi^+} = -0.065 \pm 0.015_{stat} \pm 0.010_{syst} \pm 0.002_{ext} \qquad (4)
\end{aligned}$$

If we impose the constraint between a_0 and a_2 due to analiticity and chiral symmetry [14], we obtain:

$$\begin{aligned}
CI \quad &: (a_0 - a_2) m_{\pi^+} = \quad 0.268 \pm 0.003_{stat} \pm 0.002_{syst} \pm 0.001_{ext} \\
CGKR &: (a_0 - a_2) m_{\pi^+} = \quad 0.266 \pm 0.003_{stat} \pm 0.002_{syst} \pm 0.001_{ext} \qquad (5)
\end{aligned}$$

The external error originates from the uncertainty on the branching ratio $\Gamma(K^{\pm} \to \pi^{\pm}\pi^+\pi^-)/\Gamma(\boldsymbol{K}^{\pm} \to \pi^{\pm}\pi^0\pi^0)$. Cabibbo and Isidori also assign a 5% theoretical error on $(a_0 - a_2)m_{\pi^+}$ to take into account the missing orders and the Coulomb corrections. Recent results both in radiative corrections [20] and in the next order preliminary calculations allow to decrease this contribution to the total error at 1% level.

5 Comparison and conclusions

Two statistically independent analysis have been performed by the NA48/2 collaboration to measure the $\pi\pi$ scattering lenghts: one, based on the high-statistics measurement of the $\pi^0\pi^0$ invariant mass distribution in the $\boldsymbol{K}^{\pm} \to \pi^{\pm}\pi^0\pi^0$ decay; the other, on the measurement of the phase shift variation with the $\pi^+\pi^-$ invariant mass in the $K^{\pm} \to \pi^+\pi^- e^{\pm}\nu$ decay. In Fig. 3 the agreement between these two independent measurements is shown together with other experimental results.

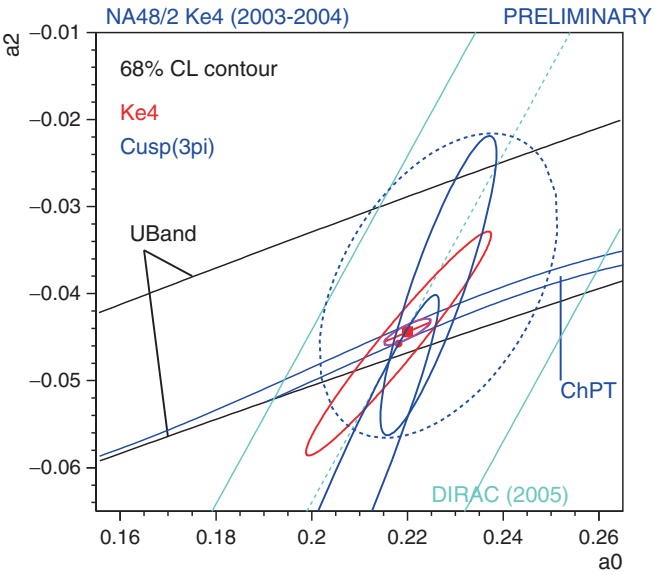

Fig. 3 Results for the $\pi\pi$ scattering lengths a_0 and a_2 in m_π^+ units. The black solid curves are the universal band boundaries and the narrow blue band is the restricted area using the ChPT constraint. The ellipses correspond to 68% CL in a two-parameter fit to $K^\pm \to \pi^\pm\pi^0\pi^0$ events (blue ellipses) and Ke4 events (red ellipse). The upper blue ellipses represent the result with the CI theory assuming a 5% (dotted) and a 1% (solid) theoretical error, respectively. The lower blue ellipse is the CGKR fit result. The red square is the result of 1-paramenter fit to Ke4 data, to be compared with the ChPT predictions (purple ellipse). The result form the DIRAC experiment (cyan) is also shown

References

1. G. Colangelo *AIP Conf. Proc.* **756**, 60 (2005).
2. M. Knecht et al., *Nucl. Phys.* **B4570**, 513 (1995).
3. L. Rosselet et al., *Phys. Rev.* **D15**, 574 (1977).
4. S. Pislak et al., *Phys. Rev. Lett.* **87**, 221801 (2001), *Phys. Rev.* **D67** 072004 (2003).
5. B. Adeva et al., [DIRAC Collaboration], *Phys. Lett.* **B619**, 50 (2005).
6. J.R. Batley et al., [NA48/2 Collaboration], *Eur. Phys. J.* **C52**, 875 (2007).
7. V. Fanti et al., [NA48 Collaboration], *Nucl. Instrum. Meth.* **A574**, 433 (2007).
8. N. Cabibbo and A. Maksymowicz, *Phys. Rev.* **B438**, 137 (1965).
9. A. Pais and S. Treiman, *Phys. Rev.* **168**, 1858 (1968).
10. G. Amoros, J. Bijnens, *J. Phys.* **G25**, 1607 (1999).
11. S. Roy, *Phys. Lett.* **B36**, 353 (1971).
12. B. Ananthanarayan, G. Colangelo, J. Gasser and H. Leutwyler, *Phys. Rep.* **353**, 207 (2001).
13. N. Fuchs, L. Girlanda and J. Stern, *Eur. Phys. J.* **C24**, 469 (2002).
14. G. Colangelo, J. Gasser and H. Leutwyler, *Nucl. Phys.* **B603**, 125 (2001).
15. J.R. Batley et al., [NA48/2 Collaboration], *Phys. Lett.* **B633**, 173 (2006).
16. N. Cabibbo, *Phys. Rev. Lett.* **93**, 121801 (2004).
17. N. Cabibbo and G. Isidori, *JHEP* **0503**, 21 (2005).
18. G. Colangelo, J. Gasser, B. Kubis and A. Rusetsky, *Phys. Lett.* **B638** 187 (2006).
19. J.R. Batley et al., [NA48/2 Collaboration], *Phys. Lett.* **B649**, 349 (2007).
20. M. Bissegger, A. Fuhrer, J. Gasser, B. Kubis and A. Rusetsky, *arXiv:087.0515*.